International Journal of Engineering Trends and Technology
ISSN: 2231-5381/ https://doi.org/10.14445/22315381/IJETT-V74I6P119

Volume 74 Issue 6, 261-268, June 2026
© 2026 Seventh Sense Research Group®

Original Article

Volcanic Activity Detection through Plume Image Analysis using CNN-LSTM

Ryan B. Jaucian[1], Alonica R. Villanueva[2]

[1,2]*Graduate Programs, Technological Institute of the Philippines, Quezon City, Philippines.*

[1]*Corresponding Author : qrbjaucian@tip.edu.ph*

Received: 25 August 2025 Revised: 24 March 2026 Accepted: 20 April 2026 Published: 27 June 2026

Abstract *- Volcanic plumes pose serious risks to aviation, public health, and the environment, and they are essential visual indicators of a volcano's eruptive activity. Effective hazard mitigation and early warning systems depend on the timely and precise classification of plume types (such as ash, steam, or gas) and the forecasting of plume direction. Convolutional Neural Networks (CNN) and Long Short-Term Memory (LSTM) algorithms are employed in this study to examine the use of a parallel machine learning model that analyzes volcanic plume imagery and predicts plume direction based on temporal and spatial features. Sequential image data was used to train the suggested parallel CNN-LSTM architecture, which allowed the model to predict directional movement over time and classify different types of plumes In addition to a directional prediction performance indicated by 0.1252 Mean Absolute Error (MAE) and 0.9217 R2, the experimental results showed high accuracy across tasks, with the model achieving a precision of 1.0000 for ash plumes, 0.9954 for steam plumes, and 0.9787 for gas plumes. The findings demonstrate the model's potential as a real-time volcanic plume monitoring application, making a substantial contribution to automated early warning systems and risk assessment techniques.*

Keywords *- Classification, Forecasting, Image Processing, Machine Learning, Plumes.*

1. Introduction

The Philippines is in a region with a high concentration of active volcanoes. This location is called the Pacific Ring of Fire (PROF) and is characterized by a large amount of tectonic activity [1]. These regions are, in fact, horseshoe-shaped and composed of nineteen (19) groups based on location and geological features. The PROF starts in the vicinity of Australia, going through Indonesia, the Philippines, Taiwan, Japan, going north to the Arctic, then going south through North America, ending in the Austral Andean volcanic Arc in South America. This large region is composed of over 400 active and dormant volcanoes spread out across different nations [2].

Research shows that countries within the area of the PROF experience a high-risk level of geological disasters. These include earthquakes, tsunamis, lahars, pyroclastic flows, and other interrelated phenomena related to volcanic activities [3]. A significant number of the inhabitants living close to or around volcanoes are always exposed to these dangers. Through modern technology, volcanologists can now predict if a volcano is going to erupt, but predicting the exact time and magnitude of the eruption is still a difficult task. For populations living near volcanoes, one of the most observable signs of volcanic activity is the presence of plumes. They serve as visual indicators of the present state of the volcano [4]. Plumes often consist of ash and pyroclastic material. These include trace gases like Sulfur Dioxide (SO_2), Carbon Dioxide, Water Vapor, and Halogens [5]. Studies have used volcanic plume datasets to analyse the effects of volcanic eruptions. For example, if the ash concentration in the atmosphere reaches a certain threshold, it can affect the local air traffic in the area. Aircraft engine parts can easily be damaged by volcanic ash [6]. A study on the December 2018 eruption of Mt. Etna showed that volcanic ash and similar gases that persisted in the atmosphere retain an almost constant altitude as far away as 400km from the volcano [7]. These also introduce contaminants into the food chain that affect the local ecosystems [8]. Researchers also found that recent volcanic eruptions around the PROF caused a significant impact on the global climate. The volcanic activity near the Tonga islands in the South Pacific produced a large enough plume that affected global weather patterns [9].

Continuous monitoring of volcanic activity is crucial for reducing disaster risk and ensuring public safety. Satellite imagery, remote sensing tools, and ground-based observations are the mainstays of traditional monitoring techniques [10-12]. In Chile, for example, volcano monitoring includes manual ash collection, analysis of gases emitted from active volcano vents, remote measurements of SO_2, and actual surface activity monitoring through web and thermal cameras.

This is an open access article under the CC BY-NC-ND license (http://creativecommons.org/licenses/by-nc-nd/4.0/)

[13]. Even though these methods yield useful data, problems such as weather, expenses, equipment, and other constraints hinder their proper application [14]. In the case of the Tagoro eruption near the Canary Islands, there was not a defined single magma chamber, which led to eruptive vents that arose either from land or sea. Monitoring and observation had been difficult, especially for submarine eruptions, because there was no visual evidence of the beginning and end of the eruption [15].

New technological developments, however, present fresh chances to improve volcanic monitoring systems [16]. To gain a better understanding of the dynamics of volcanic plumes, researchers study machine learning algorithms to leverage the growing amount of surveillance footage obtained by volcano monitoring facilities. For example, researchers in Berlin proposed a monitoring system called Monitoring Unrest from Space (MOUNTS) that used a combination of images from different satellites, terrestrial seismic data from earthquake surveillance repositories, and Artificial Intelligence (AI) to assist in volcanic activity assessment [17].

Although the application of machine learning has significantly enhanced the monitoring of volcanic activity, most studies on volcanic plumes are focused on plume identification or direction forecasting. There is limited research on integrating models that can improve the accuracy of both plume classification and prediction. To address this gap, the study designed a hybrid Convolutional Neural Network and Long Short-Term Memory (CNN-LSTM) model specifically developed for volcanic plume analysis. The CNN was used to classify spatial features, and the LSTM networks were used to predict temporal sequences. Enhancing the accuracy of volcanic plume monitoring can aid early warning systems in delivering real-time notifications and alleviate the hazardous consequences of volcanic eruptions.

2. Literature Review

2.1. Volcanic Plume Characteristics

When a volcano erupts violently, it sends out volcanic plumes, which are moving mixtures of volcanic particles, gases, and other pyroclastic materials. [18-20] The composition, density, and behavior of these plumes can change a lot depending on the type of eruption and the weather around it. The Mass Eruption Rate (MER), the composition of the magma, and the weather are all important factors [21]. The amount of material that is released into the air during a volcanic event determines the MER. The composition of the magma affects how buoyant the plume is and how many particles it has. Wind direction, wind speed, humidity, and temperature are all examples of weather variables. These weather conditions have a big effect on how plumes move through the air, how high they go, and how long they last. Several parameters are combined to estimate the amount of volcanic material ejected during eruptions. For example, the estimates of the top plume height together with the wind speed were used to develop a new radar-based statistical model that can rapidly estimate the MER during severe volcanic activities [22]. Although the accuracy of such models is still dependent on vital parameters like the wind velocity, magma composition, and volcano eruption style. Considering all of these requirements, Durig et. al. developed a decision tree in selecting the ideal model to use when estimating MER in real-time. The model to be used depends on the quality and availability of the immediate data [23].

2.2. Current Monitoring Methods

Historically, a variety of remote sensing methods have been used to monitor volcanic plumes and identify and evaluate their properties. Volcanoes are often monitored with a calibrated webcam. The Icelandic Meteorological Office uses a strategically placed network of cameras using Raspberry Pi called PiCams. They also have ArduinoCams, microcontroller-based camera modules installed in remote areas of the volcanoes where communication is difficult. This proved to be useful, especially during the 2021 Fagradalsfjall eruption [24]. Others measure gas concentrations using spectroscopic techniques [25]. We used this method on Mount Erebus to find trace gases like HCl, HF, and SO2. The results of these observations help figure out the ratios of the different parts of volcanic plumes [26]. In recent years, mobile platforms have become more common for plume observation. One study, for instance, used drone-based imaging to get a series of images that made it possible to build three-dimensional models of plume structures [27].

Satellite images are also very important for watching and studying volcanic plumes. They cover a large area and provide almost real-time observations that are necessary for finding and following eruptive events. Researchers primarily use a collection of satellite images of the same location to monitor volcanic activity, evaluate plume development, and track plume dispersion over time [28]. One study employed satellite data from Sentinel-3 to detect volcanic ash plumes ejected during the 2019 Raikoke eruption. Accurate detection was achieved by training a machine learning model with images from the 2010 Eyjafjallajökull eruption [29]. The same method is also used to monitor ground deformation caused by lava flows [30]. However, satellite images are still subject to seasonal bias. Accurate measurement of SO_2, for instance, is affected by snow cover. Large volumes of satellite data are only available during the summer months with clear skies and no snow [31]. Other studies improve on the satellite retrieval accuracy by combining outputs with other approaches, such as ground-based monitoring methods [32].

Researchers often develop specific tools for monitoring volcanic plumes. One study created a MATLAB-based algorithm to classify volcanic plumes from a dataset of visible-wavelength images. The model used image edge detection as well as thresholding to automate the classification of plume boundaries. This led to faster interpretation with

minimal external input [33]. A similar web application was developed by Grandin et. al. to estimate daily SO_2 emissions. The app lets you choose different input parameters and gives you interactive outputs to help you understand the results [34].

People also use algorithms to keep track of volcanic plumes. Trained models can often accurately predict eruption parameters such as plume height, duration, volume, and MER. Bayesian linear regression was used by one study to forecast the MER by using a dataset containing historical plume heights from the last 28 eruptions of 18 different volcanoes [35]. Convolutional Neural Network (CNN) is one of the most popular machine learning algorithms used for monitoring volcanic plumes. This is mainly because it is primarily designed to work well in semantic segmentations and image classification [36]. CNNs can accurately classify spatial features, which can be effective in identifying plume structures. Some studies have used CNN with existing video footage to sort volcanic ash particles. This makes it possible to identify ash clouds in real time during volcanic activities [37]. This technique makes volcanic plume classification faster and more accurate.

2.3. Gaps in Existing Research

Research on volcanic plumes concentrates on analyzing the spatial data of volcanic plumes. Other papers focus on the plumes' temporal data. These studies do not cover both aspects at the same time. CNNs are highly accurate in determining the spatial features in images.

The algorithm can easily identify things like texture, density, and shape. Nevertheless, CNNs have trouble modeling sequential dependencies, thus producing low results in terms of predicting plume behavior. Long Short-Term Memory (LSTM) is built to handle time-series data and is ideal for these types of tasks [38]. However, LSTMs are not designed to identify intricate spatial features in images.

Parallel CNN-LSTM models have been used in other studies, but applications are mainly focused on other fields. Most research is applied on human activity recognition, medical diagnostics, and climate modelling. Application of the CNN-LSTM to volcanic plume detection is still relatively small and limited [39-41]. Algorithms that can simultaneously process temporal and spatial features are needed to solve the difficulties encountered during volcanic eruptions. These can be seen in the ever-changing atmospheric conditions around volcanic environments or the varying plume emissions by the volcanos.

The study focused on a unified CNN-LSTM model to increase the accuracy of the model in terms of classification and forecasting. The research aims to aid in risk reduction during volcanic eruptions by enhancing early warning systems.

3. Materials and Methods

3.1. Materials

3.1.1. Hardware Specifications

The Intel i7 processor was used together with the NVIDIA GPU with Compute Unified Device Architecture (CUDA) support. These are commonly used to provide faster training for models that have large datasets. The RAM used was 16Gb and the hard drive had a 10Gb of minimum free space. Table 1 shows the hardware components used to developed the system.

Table 1. Hardware used during model development

Category	Requirement
Processor	Intel i7 10th Gen
GPU	NVIDIA with CUDA support
RAM	16GB
Disk	10GB

3.1.2. Software Specifications

Training was processed on Windows 10 and MacOS computing systems. Table 2 shows the software requirements used during the development of the model.

Table 2. Software used during model development

Category	Requirement
Programming Language	Python 3.13 or higher
Deep Learning	Latest stable PyTorch (torch)
Data Handling	Pandas (pandas) NumPy (numpy),
Visualization	Seaborn (seaborn) Matplotlib (matplotlib),
Machine Learning	Scikit-learn (scikit-learn)
Computer Vision	OpenCV (opencv-python)
Development Tools	Jupyter Notebook (notebook, ipykernel) & Visual Studio Code

The Python programming language was used in the development of the model. This was used together with PyTorch for deep learning. Numpy and Pandas were also used for numerical computations on CSV files. Matplotlib was used to generate the graphs and heatmaps.

3.2. Data Collection

Video surveillance footage from ground-based cameras is the primary dataset of the research. The 216 hours of video from volcano monitoring stations were requested from the Philippine Institute of Volcanology and Seismology (PHIVOLCS). Five thousand images were extracted from these videos using a frame sampling technique. Images were chosen based on plume visibility, representing various plume types, such as ash, steam, and gas plumes. Supplementary data were requested from publicly available repositories and similar research that deal with plume classification and prediction. These additional videos and images helped to add diversity in the dataset. The additional data introduced plume

appearances in different lighting and images in varying environmental conditions. Diverse camera angles were also added to aid in the development of the model.

3.3. Image Processing

The dataset collected for the research is composed of labelled volcanic plume images grouped into three classes. These classes are ash, steam, and gas plumes. To avoid any mistakes, only pictures that clearly showed plume structures were used. We cleaned up the image to get rid of any noise. These can happen when the image is compressed too much, the light is too low, or even when something in the environment interferes. In this step, the image was made clearer to show off the features and structures of the volcanic plumes. The images that were gathered were only manually labeled to help with the supervised learning. The annotation showed the plume's different parts.

Fig. 1 Annotated image sample

Data augmentation techniques were employed to facilitate diversity within the training dataset. The goal was to make the volcanic plumes look like they were in different kinds of weather. Some of the techniques were scaling, small rotations, changing the brightness, and even flipping the image randomly from left to right. These helped the model learn about a wider range of structures while still keeping the important parts of volcanic plumes. The model learned both the spatial and temporal features of the plume well by putting the annotated data into labelled sequences that were then sent to the CNN-LSTM algorithms. The model was trained to learn how the plumes acted over a short period of time by using a fixed sequence length of 10 timesteps. When the model was being made, the dataset was split into three parts. The first 80% was used for training, the next 10% was used for validation, and the last 10% was used for testing. To reduce noise and keep data safe, all rows with missing or infinite values were found and deleted.

3.4. Feature Extraction

Figure 2 shows a CNN-LSTM parallel architecture that was made to find the spatial and temporal features of volcanic plumes. Each algorithm processes plume features and plume patterns separately. The spatial analysis module takes spatial features out of the pictures. These are the plumes' shape, height, color, and texture. This aids the model to differentiate the varying types of volcanic plumes. The temporal analysis module calculates the changes in the plumes' features. This can be recognized through the speed of dispersion or change in size over time. The results from the spatial and temporal modules are combined to create a single feature set. This output assists the model in accurately classifying the volcanic plume type and forecasting the plume direction.

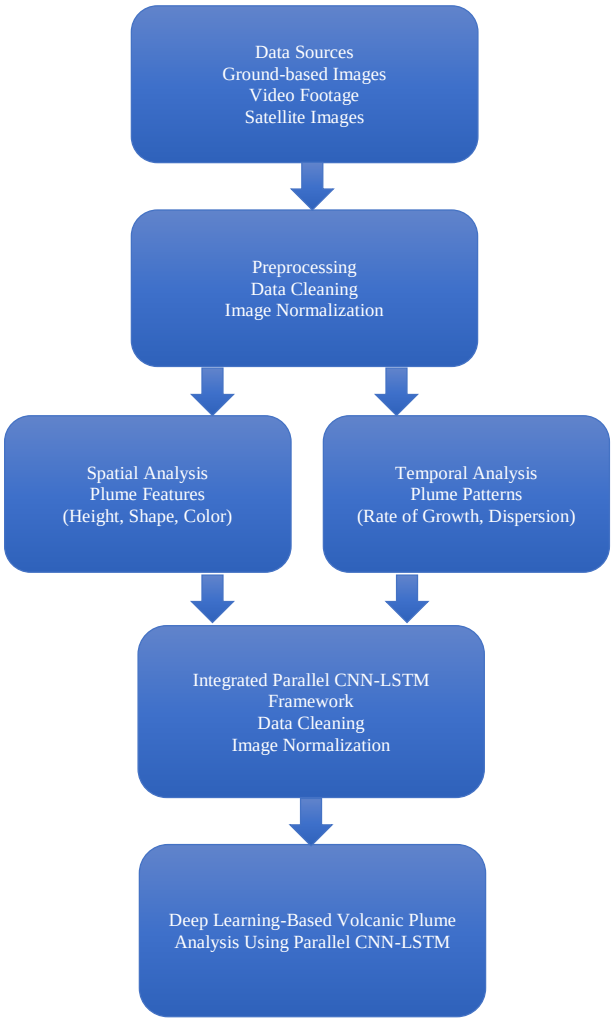

Fig. 2 CNN-LSTM parallel architecture

3.5. Training

The parallel CNN-LSTM architecture was employed to analyze volcanic plumes over a temporal sequence, as illustrated in Figure 3. Using a series of convolutional and pooling layers, the CNN model finds patterns in the images, such as the shape, size, and spread of the plume.

The LSTM model, on the other hand, learns how the plume behaves over time by looking at a series of pictures. The output from the CNN and LSTM was merged and used as input in the classification layer.

The design of the model allows it to use spatial data to classify volcanic plumes as well as temporal information to determine possible plume directions based on initial values. The parallel architecture was implemented using TensorFlow/Keras and was adjusted through the Adam optimizer. The learning rate used was 0.001 over 100 epochs during training. A batch size of 32 was implemented, as well as early stopping to prevent any overfitting. Training was stopped, and the best weights were restored if there was no improvement in the validation loss after five consecutive epochs were run.

Algorithm 1 Parallel CNN-LSTM Model

procedure INITIALIZEMODEL(input_size, hidden_size, num_layers, num_classes)
  Define CNN Branch:
    Conv1D(input_size, 64, kernel=3, stride=1, padding=1)
    ReLU Activation
    MaxPool1D(kernel=2, stride=2)
    Conv1D(64, 128, kernel=3, stride=1, padding=1)
    ReLU Activation
    MaxPool1D(kernel=2, stride=2)
    Flatten()
    Fully Connected(128)
    ReLU Activation
  Define LSTM Branch:
    LSTM(input_size, hidden_size, num_layers, batch_first=True)
    Fully Connected(128)
  Define Output Layer:
    Fully Connected(128 × 2, num_classes)
end procedure
procedure FORWARDPASS(x)
  Process Input for CNN:
    Reshape x from $(batch\_size, seq\_len, input\_size)$
      to $(batch\_size, input\_size, seq\_len)$
    Pass through CNN branch $\rightarrow out_{cnn}$
  Process Input for LSTM:
    Pass original x through LSTM $\rightarrow out_{lstm}$
    Extract last timestep output
    Pass out_{lstm} through Fully Connected Layer $\rightarrow out_{lstm}$
  Concatenate CNN and LSTM Outputs:
    Merge out_{cnn} and out_{lstm} along feature dimension
  Generate Final Output:
    Pass through Fully Connected Layer
    Obtain final output out
  Return out
end procedure

Fig. 3 Parallel CNN-LSTM algorithm

3.6. Validation

The 10% validation set was set aside to test how well the developed model could work with data that wasn't used for training. Keeping an eye on how well the model works on data it has not seen before can help you find problems with overfitting or underfitting. We also change hyperparameters and regularization techniques based on the accuracy and validation loss to make the model more stable and reliable when it comes to making predictions. Random sampling was used to keep the distribution of plume types balanced when the data was split up.

3.7. Testing

Ten percent of the full dataset was set aside for testing in order to get accurate results. The classification module's performance metrics were accuracy, precision, recall, and F1-score. The model's predictive reliability was tested using MSE, MAE, and R2. The model was checked for bias and overfitting, and changes were made so that it always gave the same results.

4. Results and Discussion

4.1. Model Performance

The high evaluation scores showed that the model could be used in systems that need to know exactly where plumes are going, especially when volcanoes are erupting. Figure 4 shows that the relationship between the training and validation loss curves steadily went down during the training process. This shows that the model was able to find the patterns in the data set. The loss values also dropped suddenly and then stayed at a lower level, which means that the model reached convergence. The close distance between the training and validation loss curves also shows that the model did not overfit or underfit. The output shows that the model produces constant results during the testing process.

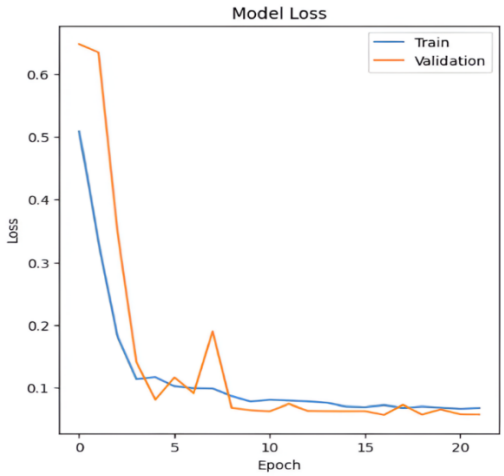

Fig. 4 Angle prediction metrics

Figure 5 shows the relationship between the actual and predicted values for the plume direction. The graphs proves that the points are clustered together forming a straight line that matches the plot line. This shows that the model is very good at predicting which way volcanic plumes will go.

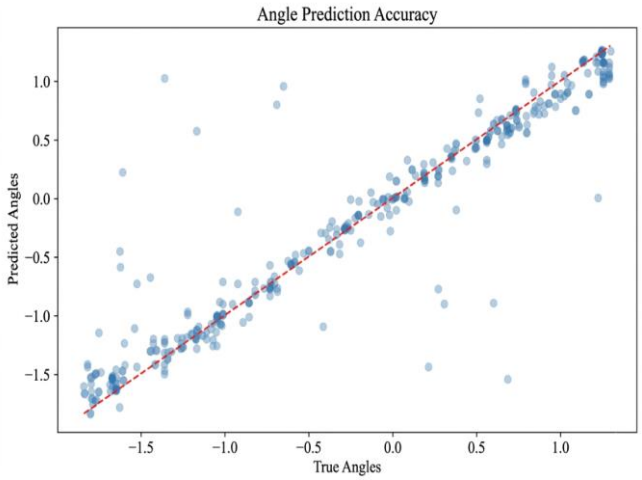

Fig. 5 Plume direction accuracy results

The MSE results of 0.0870 show the minor difference between the actual and forecasted values. This means that the model's predictions are accurate and consistent. The MAE produced a result of 0.1252, which means that the model's prediction is about 0.13 radians off from the plume's actual direction.

The model produced an R^2 score of 0.9217, which means it can identify more than 92% of the variations in the plume direction data. These different patterns in the plume direction are influenced by several factors, including the plume height, emission speed, and wind conditions. The high R^2 result is useful in determining plume behavior and predicting the possible direction of volcanic plumes.

Table 3. Plume classification results

Class	Precision	Recall	F1-Score
Ash plume	1.0000	0.7500	0.8571
Steam plume	0.9954	0.9977	0.9965
Gas Plume	0.9787	1.0000	0.9892

The research used precision, recall, and F1-score to measure the results of the model. These metrics are commonly used on imbalanced datasets or multiple classes. The tests show that all the plume types are accurately classified, as shown in Table 3. The ash plume type produced the highest score with a 1.00 for precision, 0.75 for recall, and 0.8571 for the F1-score. This means that the model was mostly right about ash plumes, but it still missed a few real ones. The model had a precision score of 0.9954, a recall score of 0.9977, and an F1-score of 0.9965 for steam plumes. This means that the model finds steam plumes with the most accuracy and consistency. The gas plume class also did very well, with a precision of 0.9787, a recall of 1.00, and an F1-score of 0.9892. This means that the model can also tell the difference between gas plumes, but not as well as it can tell the difference between steam plumes. The integrated parallel CNN-LSTM architecture enhances the performance of the developed model. Most of the research that was cited only looked at one algorithm, like CNN for plume detection. The models developed on the cited papers focus on identifying static plume characteristics. Some research extracts information from satellite images. Others used traditional image processing methods. These techniques produce low accuracy when used in varying weather conditions. On the other hand, the research integrated batch normalization, L2 regularization, and balanced the dataset to produce a more robust model. The developed model processes both the spatial and temporal features simultaneously. This approach aids the model in determining how the volcanic plumes change shape and disperse.

5. Conclusion

The outputs from the performance metrics show the robustness of the developed model. The CNN algorithm accurately identifies the plume features. Similarly, the MSE of 0.0870 showed that the LSTM algorithm produces smaller errors between data points. The developed model can use spatial and temporal processing in identifying the volcanic plumes and determine their direction. The results also showed that the model can be used with existing volcano monitoring systems. It can support making timely decisions to mitigate risk during possible volcanic eruptions.

Future research may focus on improving ash plume detection by including additional images from satellites or gas sensor readings. Supplementary data augmentation can also be done to improve accuracy.

Conflicts of Interest

The researchers declare that there is no conflict of interest relating to the publication of this research.

Funding Statement

The researchers want to thank Bicol University - Human Resource Development Program (BUHRDP) for supporting the paper.

References

[1] Tian-yu Zhang et al., "Identification and Evolution of Tectonic Units in the Philippine Sea Plate," *China Geology*, vol. 5, no. 1, pp. 96-109, 2022. [CrossRef] [Google Scholar] [Publisher Link]

[2] Biswajit Basu, and Manish Kanojia, "Modelling the Effect of Submarine Volcanic Eruption on Equatorial Oceanic Flows," *Nonlinear Analysis: Real World Applications*, vol. 74, pp. 1-13, 2023. [CrossRef] [Google Scholar] [Publisher Link]

[3] Xuecheng Li, "Impact of Geological Hazards on Regional Economic Development: Evidence from the Pacific Ring of Fire," *Frontiers in Sustainable Development*, vol. 5, no. 10, pp. 50-58, 2025. [CrossRef] [Publisher Link]

[4] Tobias Dürig et al., "REFIR- A Multi-Parameter System for Near Real-Time Estimates of Plume-Height and Mass Eruption Rate During Explosive Eruptions," *Journal of Volcanology and Geothermal Research*, vol. 360, pp. 61-83, 2018. [CrossRef] [Google Scholar] [Publisher Link]

[5] Pascal Hedelt et al., "Analysis of the Long-Range Transport of the Volcanic Plume from the 2021 Tajogaite/Cumbre Vieja Eruption to Europe using TROPOMI and Ground-based Measurements," *Atmospheric Chemistry and Physics*, vol. 25, no. 2, pp. 1253-1272, 2025. [CrossRef] [Google Scholar] [Publisher Link]

[6] Vassilis Amiridis et al., "Aeolus Winds Impact on Volcanic Ash Early Warning Systems for Aviation," *Scientific Reports*, vol. 13, no. 1, pp. 1-14, 2023. [CrossRef] [Google Scholar] [Publisher Link]

[7] Simona Scoll et al., "Multi-Sensor Analysis of a Weak and Long-Lasting Volcanic Plume Emission," *Remote Sensing*, vol. 12, no. 23, pp. 1-19, 2020. [CrossRef] [Google Scholar] [Publisher Link]

[8] Guillermo Blanco et al., "Effects of a Recent Volcanic Eruption on the Isolated Population of the Iconic Red-Billed Chough in La Palma, Canary Islands," *PeerJ*, vol. 12, 2024. [CrossRef] [Google Scholar] [Publisher Link]

[9] Marilia Hagen, and Anibal Azevedo, "Recent Volcanic Eruptions and El Niño Southern Oscillations Affecting Climate," *American Journal of Climate Change*, vol. 13, no. 4, pp. 825-844, 2024. [CrossRef] [Google Scholar] [Publisher Link]

[10] N. Carfagna et al., "Seismic Monitoring of Gas Emissions at Mud Volcanoes: The Case of Nirano (Northern Italy)," *Journal of Volcanology and Geothermal Research*, vol. 446, pp. 1-11, 2024. [CrossRef] [Google Scholar] [Publisher Link]

[11] Simone Cogliati et al., "Tracking the Behaviour of Persistently Degassing Volcanoes using Noble Gas Analysis of Pele's Hairs and Tears: A Case Study of the Masaya Volcano (Nicaragua)," *Journal of Volcanology and Geothermal Research*, vol. 414, 2021. [CrossRef] [Google Scholar] [Publisher Link]

[12] Steve A. Chien et al., "Automated Volcano Monitoring using Multiple Space and Ground Sensors," *Journal of Aerospace Information Systems*, vol. 17, no. 4, pp. 214-228, 2020. [CrossRef] [Google Scholar] [Publisher Link]

[13] Alvaro Amigo, "Volcano Monitoring and Hazard Assessments in Chile," *Volcanica*, vol. 4, no. S1, pp. 1-20, 2021. [CrossRef] [Google Scholar] [Publisher Link]

[14] Adam Cegla et al., "Detecting Volcanic Plume Signatures on GNSS Signal, based on the 2014 Sakurajima Eruption," *Advances in Space Research*, vol. 69, no. 1, pp. 292-307, 2022. [CrossRef] [Google Scholar] [Publisher Link]

[15] Carmen del Fresno et al., "The Challenge of Monitoring Volcanic Unrest Processes in Small Oceanic Islands: The Case of Tagoro Volcano (Canary Islands)," *EGU General Assembly Conference Abstracts*, pp. 19-30, 2021. [CrossRef] [Google Scholar] [Publisher Link]

[16] Giovanni Lo Bue Trisciuzzi et al., "Improved Volcanic SO_2 Flux Records from Integrated Scanning-DOAS and UV Camera Observations," *Journal of Volcanology and Geothermal Research*, vol. 455, pp. 1-14, 2024. [CrossRef] [Google Scholar] [Publisher Link]

[17] Sébastien Valade et al., "Towards Global Volcano Monitoring using Multi-sensor Sentinel Missions and Artificial Intelligence: The MOUNTS Monitoring System," *Remote Sensing*, vol. 11, no. 13, pp. 1-31, 2019. [CrossRef] [Google Scholar] [Publisher Link]

[18] Haraldur Sigurdsson, *The Encyclopedia of Volcanoes*, 2nd ed., Elsevier, 2015. [CrossRef] [Google Scholar] [Publisher Link]

[19] Congzi Xia et al., "Tracking SO_2 Plumes from the Tonga Volcano Eruption with Multi-Satellite Observations," *iScience*, vol. 27, no. 4, pp. 1-12, 2024. [CrossRef] [Google Scholar] [Publisher Link]

[20] Ryo Shingubara et al., "Development of a Drone-Borne Volcanic Plume Sampler," *Journal of Volcanology and Geothermal Research*, vol. 412, 2021. [CrossRef] [Google Scholar] [Publisher Link]

[21] Tyler Paladino et al., "Effects of Wind on the Stability of Explosive Eruption Plumes," *Journal of Volcanology and Geothermal Research*, vol. 448, pp. 1-19, 2024. [CrossRef] [Google Scholar] [Publisher Link]

[22] L. Mereu et al., "A New Radar-based Statistical Model to Quantify Mass Eruption Rate of Volcanic Plumes," *Geophysical Research Letters*, vol. 50, no. 7, pp. 1-10, 2023. [CrossRef] [Google Scholar] [Publisher Link]

[23] Tobias Dürig, Louise S. Schmidt, and Fabio Dioguardi, "Optimizing Mass Eruption Rate Estimates by Combining Simple Plume Models," *Frontiers in Earth Science*, vol. 11, pp. 1-17, 2023. [CrossRef] [Google Scholar] [Publisher Link]

[24] Talfan Barnie et al., "Volcanic Plume Height Monitoring using Calibrated Web Cameras at the Icelandic Meteorological Office: System Overview and First Application During the 2021 Fagradalsfjall Eruption," *Journal of Applied Volcanology*, vol. 12, no. 1, pp. 1-19, 2023. [CrossRef] [Google Scholar] [Publisher Link]

[25] C.R. Rowell, A.M. Jellinek, and J.T. Gilchrist, "Tracking Eruption Column Thermal Evolution and Source Unsteadiness in Ground-based Thermal Imagery using Spectral-Clustering," *Geochem Geophys Geosyst*, vol. 24, no. 11, pp. 1-45, 2023. [CrossRef] [Google Scholar] [Publisher Link]

[26] Dan Smale et al., "Opportunistic Observations of Mount Erebus Volcanic Plume Hcl, HF and SO_2 by High Resolution Solar Occultation Mid Infra-Red Spectroscopy," *Journal of Quantitative Spectroscopy and Radiative Transfer*, vol. 307, pp. 1-10, 2023. [CrossRef] [Google Scholar] [Publisher Link]

[27] Aboud Albadra et al., "Determining the Three-Dimensional Structure of a Volcanic Plume using Unoccupied Aerial System (UAS) Imagery," *Journal of Volcanology and Geothermal Research*, vol. 407, pp. 1-11, 2020. [CrossRef] [Google Scholar] [Publisher Link]

[28] V. Salgueiro et al., "Characterization of Tajogaite Volcanic Plumes Detected Over the Iberian Peninsula from a Set of Satellite and Ground-based Remote Sensing Instrumentation," *Remote Sensing of Environment*, vol. 295, pp. 1-18, 2023. [CrossRef] [Google Scholar] [Publisher Link]

[29] Ilaria Petracca et al., "Volcanic Cloud Detection using Sentinel-3 Satellite Data by Means of Neural Networks: The Raikoke 2019 Eruption Test Case," *Atmospheric Measurement Techniques*, vol. 15, no. 24, pp. 7195-7210, 2022. [CrossRef] [Google Scholar] [Publisher Link]

[30] Aggeliki Kyriou, and Konstantinos Nikolakopoulos, "Analysis of Surface Deformation During Volcanic Eruptions using Sentinel-1 Imagery," *Earth Resources and Environmental Remote Sensing/GIS Applications XIV*, vol. 12734, 2023. [CrossRef] [Google Scholar] [Publisher Link]

[31] Vitali E. Fioletov et al., "Estimation of Anthropogenic and Volcanic SO_2 Emissions from Satellite Data in the Presence of Snow/Ice on the Ground," *Atmospheric Measurement Techniques*, vol. 16, no. 22, pp. 5575-5592, 2023. [CrossRef] [Google Scholar] [Publisher Link]

[32] Can Li et al., "A New Machine-Learning-based Analysis for Improving Satellite-Retrieved Atmospheric Composition Data: OMI SO_2 as an Example," *Atmospheric Measurement Techniques*, vol. 15, no. 18, pp. 5497-5514, 2022. [CrossRef] [Google Scholar] [Publisher Link]

[33] Riccardo Simionato et al., "Plumetrap: A New MATLAB-based Algorithm to Detect and Parametrize Volcanic Plumes from Visible-Wavelength Images," *Remote Sensing*, vol. 14, no. 7, pp. 1-23, 2022. [CrossRef] [Google Scholar] [Publisher Link]

[34] Raphaël Grandin et al., "Automatic Estimation of Daily Volcanic Sulfur Dioxide Gas Flux from TROPOMI Satellite Observations: Application to Etna and Piton de la Fournaise," *JGR Solid Earth*, vol. 129, no. 6, pp. 1-30, 2024. [CrossRef] [Google Scholar] [Publisher Link]

[35] Mark J. Woodhouse, "Estimating the Mass Eruption Rate of Volcanic Eruptions from the Plume Height using Bayesian Regression with Historical Data: The MERPH Model," *Journal of Volcanology and Geothermal Research*, vol. 454, pp. 1-13, 2024. [CrossRef] [Google Scholar] [Publisher Link]

[36] T.C. Wilkes, T.D. Pering, and A.J.S. McGonigle, "Semantic Segmentation of Explosive Volcanic Plumes Through Deep Learning," *Computers and Geosciences*, vol. 168, pp. 1-14, 2022. [CrossRef] [Google Scholar] [Publisher Link]

[37] José Francisco Guerrero Tello et al., "Convolutional Neural Network Algorithms for Semantic Segmentation of Volcanic Ash Plumes using Visible Camera Imagery," *Remote Sensing*, vol. 14, no. 18, pp. 1-18, 2022. [CrossRef] [Google Scholar] [Publisher Link]

[38] D. Z. Haq et al., "Long Short-Term Memory Algorithm for Rainfall Prediction based on El-Nino and IOD Data," *Procedia Computer Science*, vol. 179, pp. 829-837, 2021. [CrossRef] [Google Scholar] [Publisher Link]

[39] Maria Pia Del Rosso et al., "On-Board Volcanic Eruption Detection through CNNs and Satellite Multispectral Imagery," *Remote Sensing*, vol. 13, no. 17, pp. 1-16, 2021. [CrossRef] [Google Scholar] [Publisher Link]

[40] Weiwei Bai et al., "Cooperative Spectrum Sensing Method based on Channel Attention and Parallel CNN-LSTM," *Digital Signal Processing*, vol. 158, 2025. [CrossRef] [Google Scholar] [Publisher Link]

[41] Zhonghe Tian et al., "A Paralleled CNN and Transformer Network for PPG-based Cuff-Less Blood Pressure Estimation," *Biomedical Signal Processing and Control*, vol. 99, 2025. [CrossRef] [Google Scholar] [Publisher Link]

[42] Burak Gülmez, "Stock Price Prediction using the Sand Cat Swarm Optimization and an Improved Deep Long Short Term Memory Network," *Borsa Istanbul Review*, vol. 24, pp. 32-46, 2024. [CrossRef] [Google Scholar] [Publisher Link]